This is an open access article published under an ACS AuthorChoice License, which permits copying and redistribution of the article or any adaptations for non-commercial purposes.

ACS OMEGA

Article

Cite This: ACS Omega 2018, 3, 12341−12348

http://pubs.acs.org/journal/acsodf

Anthracene-Based Highly Selective and Sensitive Fluorescent "*Turn-on*" Chemodosimeter for Hg^{2+}

Chinna ayya swamy P,*[,†] Jeyabalan Shanmugapriya,[‡] Subramanian Singaravadivel,[§] Gandhi Sivaraman,*[,∥] and Duraisamy Chellappa[∥]

[†]Schulich Faculty of Chemistry Technion City, Haifa 32000, Israel

[‡]Department of Chemistry, Thiagarajar College of Engineering, Madurai 625 015, India

[§]Department of Chemistry, SSM Institute of Engineering and Technology, Dindigul 624002, India

[∥]School of Chemistry, Madurai Kamaraj University, Madurai 625021, India

Supporting Information

ABSTRACT: Three π-extended anthracene-bearing thioacetals (**1**−**3**) have been synthesized, and their fluorescence "*turn-on*" responses to Hg^{2+} ions are studied. The chemodosimetric fluorescence-sensing behavior and their resulting hydrolysis via a desulfurization reaction mechanism leads to the formation of highly fluorescent respective aldehyde substitutions. Furthermore, this mechanism was supported by increase in the quantum yields of their resulting aldehydes and is correlated to their molecular substitution. The chemosensors **1**−**3** have exhibited to be promising receptors toward Hg^{2+} ions in the presence of other competitive metal ions. Moreover, the detection limits of **1**−**3** have been found to be in the nanomolar range (94, 59, and 235, respectively). Fluorescence microscopic imaging studies show that **1**−**2** have been found to be effective for fluorescence imaging in live cells. Moreover, compounds **1**−**3** act as potential candidates for the detection of Hg^{2+} in environmental and biological systems as well as real samples.

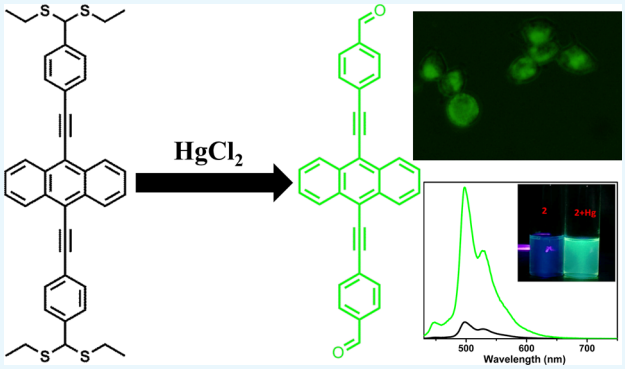

INTRODUCTION

The selective detection of toxic metal ions (heavy metals) has been receiving much attention because of their effect on health and the environment.[1] Recent results from the U.S. Environmental Protection Agency and the International Agency for Research show that the heavy metals cause cancer and are called as carcinogens.[2] Among all other heavy metal ions, mercury is more toxic even when present in small quantities, and it has engendered not only from geological events but also from human activities.[3] There are serious health problems associated with mercury pollution, as it can reach the vital organs of humans in several ways and leads to deadly diseases such as acrodynia (pinks disease), Hunter-Russell syndrome, and Minamata disease. Moreover, mercury forms strong complexes with sulfur-containing biomolecules and leads to the malfunction of proteins and enzymes. Consequently, it results in a wide variety of diseases related to the kidney, brain, and central nervous system damage.[4] Thus, selective and sensitive on-site recognition of mercury ions is crucial in environmental protection and health monitoring. Several traditional analytical methods are available for the identification and detection of Hg^{2+} ions and they include atomic absorption spectroscopy, inductively coupled plasma spectroscopy, molecular absorption spectroscopy, and electroanalytical techniques. Nevertheless, these sophisticated instrumental methods often involve significant sample preparation and expensive laboratory-based instrumentation.[5] Recently, fluorescence spectroscopic methods have gained much interest because of better sensitivity, response, and ease in sample preparation.[6]

Numerous findings have been reported on the fluorogenic response-based detection of Hg^{2+} ions by employing important strategies such as complexation,[7] xanthene ring opening,[8] desulfurization,[9] cyclization,[10] Hg^{2+}-promoted deprotection of thioacetals,[11a−d] use of chemodosimeters,[11e,f] and so on. It is known that the synthesis of thioacetals occurs via protection of aldehydes or ketones by thiols and deprotection could be achieved only upon addition of Hg^{2+} ions. Therefore, this type of reactions might be employed for selective detection of Hg^{2+} ions. Aldehyde is well known as a strong electron-withdrawing group, which once protected by alkyl thioacetal groups forms moieties that might be regarded as electron donors. Hence, the selective and ratiometric luminescent probe for Hg^{2+} could be achieved by deprotection of the thioacetal, by using intra-

Received: May 26, 2018
Accepted: September 18, 2018
Published: October 1, 2018

© 2018 American Chemical Society

DOI: 10.1021/acsomega.8b01142
ACS Omega 2018, 3, 12341−12348

Scheme 1. Synthetic Scheme for Compounds 1−6

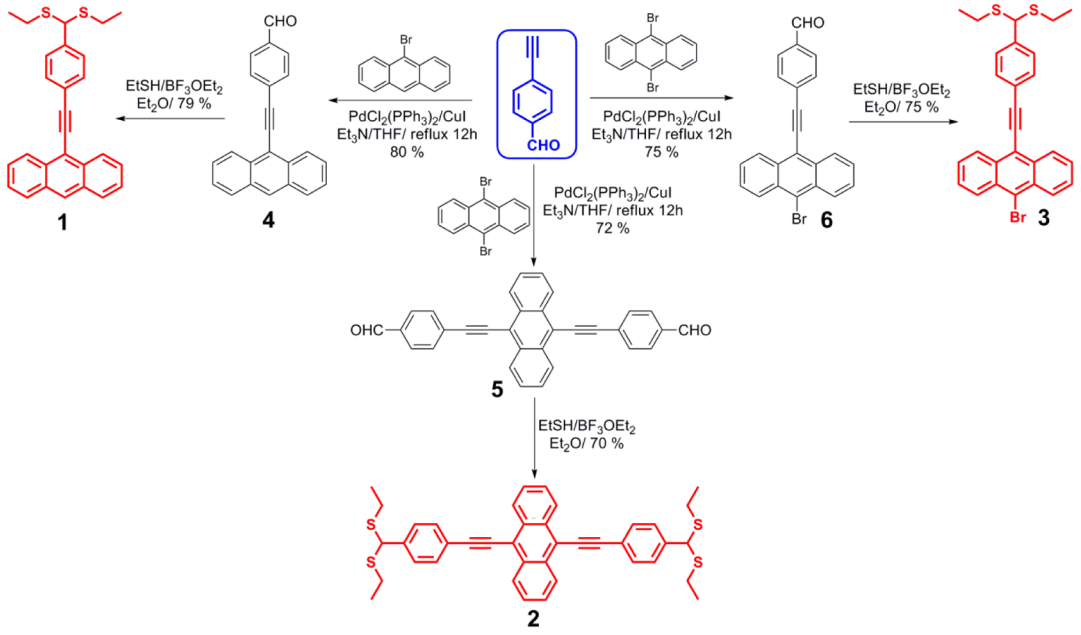

molecular charge transfer (ICT) or photon-induced electron transfer (PET) as a signaling tool, in which the fluorophore unit would act as the electron donor, whereas the aldehyde group might be the electron acceptor. As expected, the addition of Hg^{2+} ions to thioacetal leads to deprotection and subsequently, the electronic properties of the product and reactant are changed. This leads to the change in the ICT or PET process before and after the deprotection of thioacetals, resulting in a change of fluorescence emission. On the basis of this phenomenon, several colorimetric or fluorometric chemosensors for Hg^{2+} have been developed including thioacetal derivatives of triphenylamine,[12] coumarins,[13] perylene diimide,[14] boron-dipyrromethene,[15] tetraphenylethylene,[16] and 1,8-naphthalimide.[17] However, π-extended anthracene thioacetal-based chemosensors for Hg^{2+} are rarely reported in the literature. Here, taking advantage of the fluorescence behavior of anthracene three new anthracene-containing thioacetals have been designed, **1**−**3**, obtained from the reaction of aldehydes (**4**−**6**) (which emit green luminescence upon excitation) with ethanethiol in the presence of Lewis acid. These innovative anthracene-containing thioacetals are shown to be selective chemodosimeters for Hg^{2+} in a tetrahydrofuran (THF)/phosphate-buffered saline (PBS) (1:1, v/v, pH 7.4) solution and in living cells. These new probes show bright emission after the addition of an aqueous solution of Hg^{2+} ions and it is also complemented by an enhanced fluorescence color change. These changes are noticeable by the naked eyes under normal illumination. Moreover, these new probes are found as exceedingly selective and sensitive receptors for Hg^{2+} ions, even in the presence of competitive metal ions.

RESULTS AND DISCUSSION

Synthesis and Characterization. The synthetic scheme for compounds **1**−**6** is shown in Scheme 1. Compounds **4**−**6** are synthesized by the Sonogashira cross-coupling reaction[18] between the bromo derivatives of anthracene and 4-ethynyl benzaldehyde (72−80%). Compounds **1**−**3** have been obtained from **4**−**6** via Lewis acid[19]-catalyzed thioacetal formation, respectively (70−79%). This synthetic route is found to be much easier with a simple method of purification and is reliable for large-scale production of target compounds. Compounds **1**−**6** are characterized using ^{1}H, ^{13}C NMR, and high-resolution mass spectrometry (HRMS). Furthermore, compound **5** has been structurally confirmed by single crystal X-ray diffraction (Figure 1). The parameters associated with the crystal data are shown in Table S1.

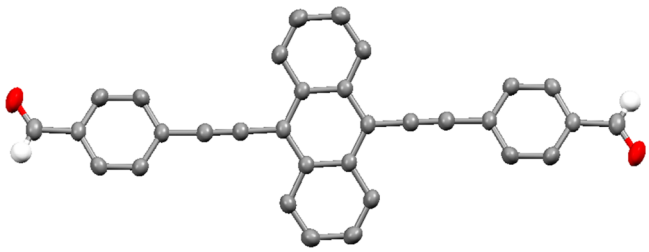

Figure 1. Molecular structure of **5** omitting all hydrogen atoms for clarity.

Photophysical Properties. The optical studies of freshly prepared compounds **1**−**3** are performed in THF/PBS (1:1, v/v, pH 7.4) buffer and they are shown in Figure 2. Compounds **1**−**3** have displayed two major absorption events in the region of 390 to 445 nm, whereas emission bands are identified in the span of ∼430−515 nm (Table 1 and Figure 2). The absorbance and luminescence bands of **2** have exhibited a significant red shift compared to **1** and **3**, owing to the presence of two acetylene units, which lead to increase its conjugation. However, the emission intensity and quantum yield of **2** (3%) have been found to be very weak compared to **1** (20%) and **3** (10%). It might be due to the PET process from the thioacetal to the fluorophore (anthracene) as well as flexibility around the thioacetal moiety. Hence, the increase in the flexibility and heavy metal content in the molecular systems leads to decrease in the fluorescence quantum yield.

Absorption and Fluorescence Studies of 1−3 toward Various Metal Ions. To gain quantitative insights into the sensitivity and selectivity of freshly prepared compounds **1**−**3**

DOI: 10.1021/acsomega.8b01142
ACS Omega 2018, 3, 12341−12348

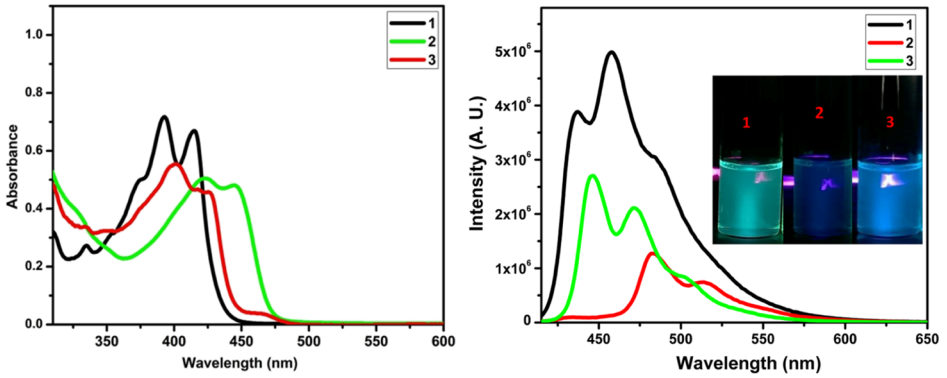

Figure 2. Absorption (left) and luminescence spectra (λ_{ex} = 400 nm) (right) of **1**−**3** in THF/PBS buffer (1:1, v/v, pH 7.4) (1 μM); (insets): photographs of compounds **1**−**3** under UV light (365 nm).

Table 1. Optical Data of 1, 2, and 3[a]

compounds	absorbance (nm)/ε	luminescence (nm)	quantum yield[b] (%)
1	390 (7.2 × 10^5), 410 (7.2 × 10^5)	437, 455	19.85 ± 0.22[c]
2	415 (5.1 × 10^5), 438 (4.8 × 10^5)	490, 515	2.1 ± 0.19
3	400 (5.6 × 10^5), 420 (4.6 × 10^5)	446, 470	8.58 ± 0.23
1 + Hg2+	394 (9.0 × 10^5), 415 (8.4 × 10^5)	435, 460	30.76 ± 0.57
2 + Hg^{2+}	425 (5.8 × 10^5), 445 (7.2 × 10^5)	495, 530	85.77 ± 0.22
3 + Hg^{2+}	405 (7.1 × 10^5)	445, 470	13.42 ± 0.24

[a]All given data are for 1 μM of a 1.1 ratio of THF/PBS buffer solutions. [b]Quantum yields are calculated using quinine sulfate (0.1 M in H_2SO_4, Φ_F = 57.7%) solution as reference and using the following formula $\Phi = \Phi_F \times I/I_R \times A_R/A \times \eta^2/\eta_R^2$ where Φ = quantum yield, I = intensity of emission, A = absorbance at λ_{ex}, η = refractive index of solvent. [c]The quantum yields of compounds are determined in a 1.1 ratio of THF and PBS buffer and the standard error is equal to the standard deviation of five independent measurements.

toward Hg^{2+} ions, UV−vis absorption and fluorescence studies have been performed in THF/PBS buffer (1:1, v/v, pH 7.4) (Table 1). Upon addition of Hg^{2+} ions to **1**−**3**, rational changes have been observed in the absorption bands. The absorption bands of **1**−**3** at 390, 415, and 400 nm have gradually increased and they have displayed a slight shift to the bathochromic region. It indicates that the Hg^{2+} ions are tangling the thioacetal moieties and convert them into formyl groups. The saturation of **1**−**3** is reached upon the addition of only two equivalents for **1** or **3** and three equivalents for **2** of Hg^{2+} ions. However, the absorption profiles of **1**−**3** show similar behavior compared to their precursors **4**−**6** upon the addition of excess Hg^{2+} ions, by evidencing strongly that the dithioacetal in **1**−**3** has been completely transformed into aldehyde in the presence of Hg^{2+} ions.

As mentioned earlier, compounds **1**−**3** have displayed weak fluorescence because of the presence of a heavy atom effect as well as the PET process that occurred from the dithiane (sulfur atom) to the π-anthracene group. However, the fluorescence intensity has been gradually enhanced by addition of Hg^{2+} with a 1:1 ratio of THF and PBS buffer solution of **1**−**3**. For example, the weak fluorescence emission of **1** at 455 nm has been gradually enhanced and simultaneously was red-shifted to appear at 460 nm (a twofold intensity increment). It reaches saturation when 2.0 equiv of Hg^{2+} is added. The new bright fluorescent emission at 460 nm indicates a new species formation such as the aldehyde. Similarly, compound **2** has exhibited very weak emission at 515 nm and showed strong bright green emission at 530 nm (10-fold intensity increment) upon addition of Hg^{2+} ions (Figure 3). However, **3** has shown

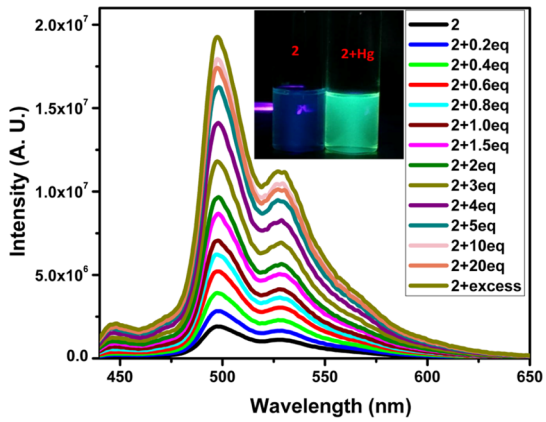

Figure 3. Fluorescent spectral changes associated with **2** (1 μM) after successive addition of Hg^{2+} ions in THF/PBS buffer (1:1, v/v, pH 7.4) (λ_{ex} = 400 nm).

minimal changes in emission intensity, after addition of Hg^{2+} and it has been attributed to the heavy atom effect of bromine (heavy atom effect dominated by PET).

Moreover, good agreement with linear fitting is observed between the concentration of Hg^{2+} ions (0−2.5 μM) and the luminescence intensity (SI), and it enables to quantify the relevant concentration of Hg^{2+} via compounds **1**−**3**. Furthermore, the detection limits of **1**−**3** toward Hg^{2+} are found to be 9.5 × 10^{-8}, 5.9 × 10^{-8}, and 23.5 × 10^{-8} M, respectively[20] by using the well-known equation, LOD = 3 SD/slope, and the limit of quantification has been obtained using the equation, LOQ = 10 SD/slope, where SD is the standard deviation from the blank measurement and the slope is obtained from the calibration curve of the standard (Table S2). The detection limit of **2** is found to be much lower compared to the literature reports, whereas other two probes (**1** and **3**) have shown similar detection limits in accordance with the observations noted for Hg^{2+} reported elsewhere[20] (Table S3).

Furthermore, the fluorescence responses of **1**−**3** have been investigated toward various metal ions and compared with Hg^{2+} ions (Figure 4). Solutions of **1**−**3** (1 μM) in THF/PBS

DOI: 10.1021/acsomega.8b01142
ACS Omega 2018, 3, 12341−12348

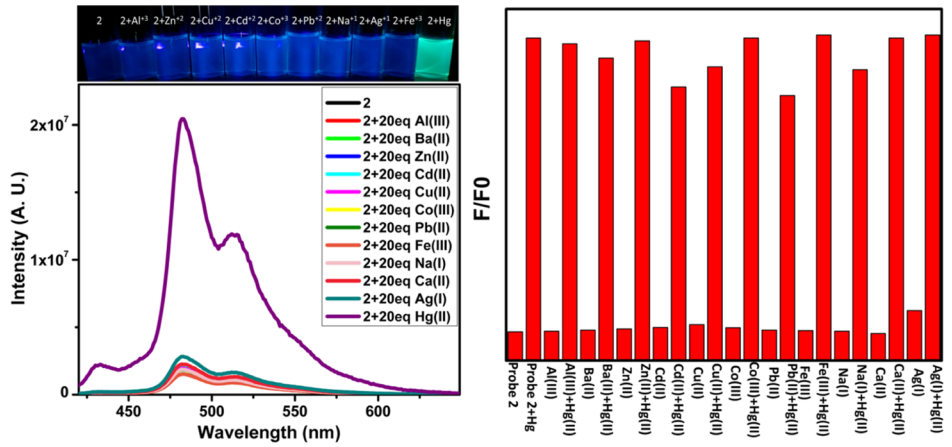

Figure 4. Emission spectra of **2** (1 μM) in THF/PBS (1:1, v/v, pH 7.4) in the absence or presence of 20 equiv of Na^+, K^+, Co^{2+}, Cu^{2+}, Ag^+, Pb^{2+}, Ba^{2+}, Fe^{3+}, Zn^{2+}, Al^{3+}, Cd^{2+}, and Hg^{2+} (λ_{ex} = 400 nm). Inset: Digital photograph of **2** (10 μM) in the absence or presence of various metal ions under a portable UV lamp at 365 nm (left). Fluorescence enhancement (F/F_0) at 495 nm of **2** (1 μM) toward various metal ions with Hg^{2+} (20 μM) and other metals only (40 μM) (right).

buffer (1:1, v/v, pH 7.4) are treated with 20 equiv and more of several different metal ions such as Na^+, K^+, Co^{2+}, Cu^{2+}, Ag^+, Pb^{2+}, Ba^{2+}, Fe^{3+}, Zn^{2+}, Al^{3+}, and Cd^{2+} for the investigation of selectivity. Probes **1**−**3** have displayed high selectivity toward Hg^{2+} ions, whereas there is no change in luminescence emission bands, even after the addition of excess amount of other metal ions. However, a very small increment has been observed in fluorescence intensity, when 20 equiv of Ag^+ is added to **1**−**3**. It might be due to the interaction of thioacetal moiety and Ag^+ induces emission enhancement. Moreover, the coordination of Ag^+ ion with thioacetal moiety of **1**−**3** prevents the PET quenching process and it leads to restoration of emission.[21] Further, the fluorescence responses of **1**−**3** have been examined toward the addition of Hg^{2+} ions in the presence of various potentially competing species, for example, Na^+, K^+, Co^{2+}, Cu^{2+}, Ag^+, Pb^{2+}, Ba^{2+}, Fe^{3+}, Zn^{2+}, Al^{3+}, and Cd^{2+}. Probes **1**−**3** are moderately interacting with 20 equiv of Ag^+, whereas the initial fluorescence intensities of **1**−**3** are not changed upon the addition of 20 equiv and more of different other metal ions (Figure 4). However, subsequently, the addition of 2 equiv or 3 equiv of Hg^{2+} ions solution has elicited a prominent fluorescence enhancement, which further has demonstrated that compounds **1**−**3** have shown exceptional selectivity for Hg^{2+} ions in the presence of other above-mentioned competing species. Notably, the enhanced fluorescence response renders compounds **1**−**3** as selective and sensitive receptors for Hg^{2+} via simple visual-eye investigation even in the presence of various other metal analytes. Thus, the present absorption and fluorescence studies clearly demonstrate that **1**−**3** might be applicable as selective fluorescence "*turn-on*" chemodosimeters for Hg^{2+} ions over other biologically important metal ions.

To evaluate the fluorescence changes with respect to time, the study of 1 μM **1** or **2** has been carried out in the presence of Hg^{2+} ions at different time intervals. The results reveal that the total fluorescence intensity gain of **1** and **2** has been achieved toward Hg^{2+} in less time, merely 5 min by indicating that these probes are applicable to real-time monitoring of Hg^{2+} (Supporting Information). Moreover, for efficient detection of biologically important metal ions in a biological system, the sensor should work in the range of biological pH. The emission profiles of compounds **1** and **2** are found invariant with respect to any change in pH (3.0−10), thus promising for the recognition of Hg^{2+} ions in biological samples (Supporting Information).[22]

In order to evaluate the structural aspects along with the sensing mechanism of probes **1**−**3** with Hg^{2+} ions, ^{1}H NMR titration experiments are performed in the presence and absence of Hg^{2+} in DMSO-d_6 and they have provided quick evidence. By the addition of 2 equiv of Hg^{2+} ions with **1**, the representative proton signal consistent to methine proton of the thioacetal group has exclusively disappeared at 4.98 ppm, along with the appearance of a new signal at 10.36 ppm, which is assigned for the −CHO group (Supporting Information). Similar behavior has been observed for other two probes (**2**−**3**) with Hg^{2+} ions. On the basis of these results, it is strongly believed that the successful deprotection reaction of probes **1**−**3** has been triggered by Hg^{2+} ions. Furthermore, the HRMS spectral analysis of **1**−**3** has displayed molecular ion peaks at m/z = 413.1330, 649.2066, and 493.0464, respectively, and by the addition of excess Hg^{2+} ions, they are changed to m/z = 307.1117, 435.1370, and 385.0304. This is same as for **4**−**6** (Figures S7−S10, Supporting Information) and it confirms the deprotection of thiols in the presence Hg^{2+} ions, by producing free aldehyde groups with bright luminescence.

To get insight into the changes in photophysical properties of **1**−**3** before and after the addition of Hg^{2+} ions, the density functional theory (DFT) calculations are accomplished with the B3LYP-6-311G basis set by using the Gaussian 03 program.[23] The frontier molecular orbitals of **1**−**3** are mainly localized on the π-conjugated anthracene unit. The highest occupied molecular orbital (HOMO) of compound **1** is localized on the anthracene unit, whereas the lowest unoccupied molecular orbital (LUMO) spreads over the aldehyde units. It gives a strong evidence of enhancement in fluorescence via the ICT process [π-conjugated (anthracene) unit to −CHO] upon the addition of Hg^{2+} ions. On the other hand, a DFT study of **2** shows that the HOMO and LUMO are localized only on the π moiety of anthracene unit and hence, the enhancement of fluorescence occurs via the absence of PET upon the addition of Hg^{2+} ions. From these studies, one can tentatively conclude that the emission enrichment in **1** occurs via ICT over PET, whereas it occurs in **2** via the absence of PET.

DOI: 10.1021/acsomega.8b01142
ACS Omega 2018, 3, 12341−12348

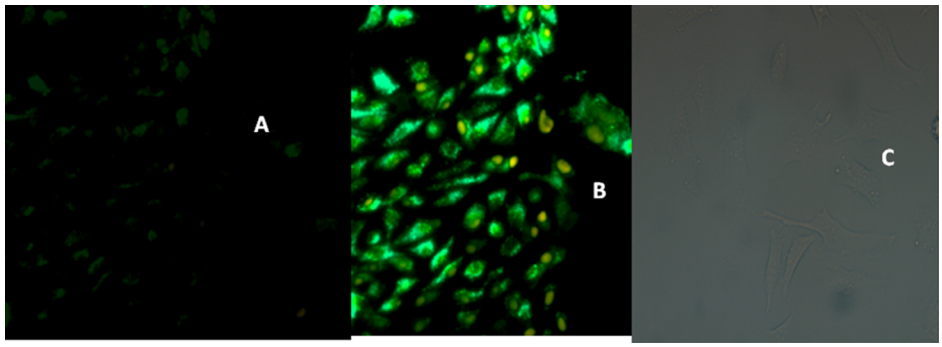

Figure 5. Fluorescence imaging of Hg^{2+} in HeLa cells at 37 °C (a) bright field image of **2** + Hg^{2+} ions-treated HeLa cells; (b) fluorescence imaging of HeLa cells with compound **2** after 10 min of treatment of 10 μM Hg^{2+} ions; (c) HeLa cells incubated with **2** for 30 min.

Additionally, to evaluate the recognition of Hg^{2+} in biological cellular media by using synthesized probes **1** and **2**, fluorescence cellular imaging has been performed in PBS containing 20% DMSO. First, HeLa cells are incubated with 10 μM of probes **1** or **2** in PBS for 30 min at 37 °C, and are found to be nonfluorescent (Figure 5). However, upon the addition of Hg^{2+} ions with the cells preloaded with **1** and **2**, the entire cells have displayed exceptional green luminescence enrichment in the intracellular area. These bioimaging experiments of **1** and **2** have provided valuable information not only about cell permeability and biocompatibility but also the effectiveness of the probes for cellular imaging. On the basis of these results, one can conclude that probe **1** or **2** is a promising and successful chemodosimeter for Hg^{2+} ions in living organisms.

CONCLUSIONS

In summary, rationally designed anthracene-based thioacetals have been synthesized and their luminescence chemosensory behaviors are studied toward Hg^{2+} ions. Probes **1**−**3** are proven to possess excellent selectivity and sensitivity and as luminescent "*turn-on*" probes for the recognition of Hg^{2+} ions over various metal ions. Compound **2** demonstrates faster (less than 5 min) "*turn-on*" fluorescence response and it is found to have very low limit of detection toward Hg^{2+} ions than **1** in THF/PBS (1:1, v/v, pH 7.4) buffer media. The fluorescence intensities of **1**−**2** do not vary even in the wide range of pH (3−10) and thus, they could be useful for the recognition of Hg^{2+} in a biological cellular medium. Probes **1**−**2** have proved to be biocompatible and successful for intracellular fluorescence imaging of Hg^{2+} ion, and they lead to potential applications in biology.

EXPERIMENTAL SECTION

Unless stated otherwise, all chemicals and solvents were purchased from commercial sources and used without further purification. Reactions were carried out using oven-dried glassware. Flash chromatography was carried out on Merck Kieselgel 60 (230−400 mesh) as the stationary phase under a positive pressure using AR grade solvents; the procedure includes removal of solvents under reduced pressure. Thin-layer chromatography was performed on precoated Merck Kieselgel silica gel plates (60 F254, Merck, Germany) monitored by UV light and Iodine. Nuclear magnetic resonance (NMR) spectra were recorded on Bruker AVANCE 400 spectrometers. Chemical shifts for ^{1}H and ^{13}C NMR are referenced to the residual solvent resonance and chemical shifts are reported in parts per million (ppm) from high to low frequency. *J*-values are reported for ^{1}H NMR coupling constants in the unit of hertz (Hz). The residual solvent signals were used as references and the chemical shifts were converted to the TMS (tetramethylsilane) scale: $CDCl_3$: δ_H = 7.26 ppm, δ_C = 77.16 ppm, DMSO-d_6: δ_H = 2.50 ppm, δ_C = 39.51 ppm. The following abbreviations or combinations thereof were used to explain the multiplicities: s = singlet, d = doublet, t = triplet, q = quartet, qu = quintet, m = multiplet, br = broad. High-resolution electrospray ionization mass spectrometry was performed with a Water Micromass LCT Premier instrument. The single crystals were mounted on a Nonius Kappa CCD diffractometer (**5**) and data were collected using graphite-monochromatized Mo Kα-radiation (Å = 0.71073) at 293 K (**5**). The following programs were used for data collection and reduction:Nonius 1997 Collect, HKLDENZO, and Scalepack.[24] The structures were solved by direct methods using the program package maXus and refined in the usual way using SHELXL97.[25] Nonhydrogen atoms were refined anisotropically and hydrogen atoms isotropically. CCDC: 1842083

Synthesis of 1. To a solution of **4** (0.2 g, 0.08 mmol) in dry Et_2O (15 mL) under the N_2 atmosphere, 5 μL of $BF_3{\cdot}Et_2O$ (0.04 mmol) was added. To this, ethanedithiol (90 mg, 0.09 mmol) was added slowly dropwise at room temperature (RT). The reaction mixture was stirred at RT for 12 h. The solvent was evaporated under vacuum and the residue was extracted using EtOAc. The organic layer was washed with H_2O several times followed by washing with saturated NaCl solution. The organic layer was dried over anhydrous Na_2SO_4 and the solvent was removed under reduced pressure. The residue was purified via column chromatography (Silica gel, 2:8 (v/v) EtOAc: hexanes as eluent) to obtain **1** as an orange solid. Yield: 79% ^{1}H NMR (400 MHz $CDCl_3$): δ 8.64 (m, 2H), 8.44 (s, 1H), 8.02 (d, *J* = 8 Hz, 2H), 7.74 (d, *J* = 8 Hz, 2H), 7.56 (m, 6H), 7.52 (m, 2H), 4.98 (s, 1H), 2.60 (m, 4H), 1.26 (t, *J* = 7.6 Hz, 6H). ^{13}C NMR (100 MHz $CDCl_3$) 141.0, 132.7, 131.8, 131.2, 128.7, 128.0, 127.8, 126.7, 125.7, 123.0, 100.4, 86.7, 52.3, 26.3, 14.4. HRMS: $[M + H]^+$ calcd for $C_{27}H_{25}S_2$, 413.1392; found $[M + H]^+$, 413.1330.

Synthesis of 2. Compound **2** was prepared following a procedure similar to that used for compound **1**. The quantities involved and characterization data are shown below; **5** (0.5 g, 1.15 mmol), ethanedithiol (0.27 g, 2.87 mmol), $BF_3{\cdot}Et_2O$ (81 μL, 0.57 mmol) dry Et_2O (25 mL). Yield: 70%. ^{1}H NMR (400 MHz $CDCl_3$): δ 8.67 (m, 4H), 7.74 (d, *J* = 8 Hz, 2H), 7.64 (m, 4H), 7.55 (d, *J* = 8 Hz, 2H), 4.99 (s, 2H), 2.61 (m, 8H), 1.26 (t, *J* = 7.6 Hz, 12H). ^{13}C NMR (100 MHz $CDCl_3$) 141.3, 132.1, 131.8, 128.0, 127.3, 126.9, 122.8, 118.5, 102.2, 86.9,

DOI: 10.1021/acsomega.8b01142
ACS Omega 2018, 3, 12341−12348

52.3, 26.3, 14.4. HRMS: $[M + H]^+$ calcd for $C_{40}H_{41}S_4$, 649.2091; found $[M + H]^+$, 649.2066.

Synthesis of 3. Compound **3** was prepared following a procedure similar to that used for compound **1**. The quantities involved and characterization data are shown below; **6** (0.5 g, 1.30 mmol), ethanedithiol (0.15 g, 1.63 mmol), $BF_3{\cdot}Et_2O$ (115 μL, 0.57 mmol) dry Et_2O (25 mL). Yield: 75%. ^{1}H NMR (400 MHz DMSO-d_6): δ 8.68 (m, 2H), 8.56 (m, 2H), 7.73 (d, J = 8 Hz, 2H), 7.76 (m, 2H), 7.53 (d, J = 8 Hz, 2H), 4.99 (s, 1H), 2.58 (m, 4H), 1.26 (t, J = 7.6 Hz, 6H). ^{13}C NMR (100 MHz DMSO-d_6) 141.2, 132.9, 131.7, 130.2, 128.2, 127.9, 127.4, 127.1, 126.8, 124.2, 122.7, 118.0, 101.4, 86.3, 52.2, 22.6, 14.7. HRMS: $[M + H]^+$ calcd for $C_{27}H_{23}S_2Br$, 491.0497; found $[M + H]^+$, 491.0479.

Synthesis of 4. A solution of 4-ethynylbenzaldehyde (0.5 g, 3.84 mmol), 9-bromoanthracene (1.24 g, 4.81 mmol), CuI (0.058 g, 0.31 mmol), and $Pd(PPh_3)_2Cl_2$ (0.13 g, 0.09 mmol) in dry triethylamine (25 mL) and THF (40 mL) was placed in a flask and degassed by freeze and pump three to four times. The reaction mixture was warmed and refluxed for 24 h, the solvent was removed under reduced pressure, and crude product was extracted by dichloromethane/water and was purified by column chromatography (SiO_2, petroleum ether/EtOAc = 10:1) to afford compound **4** (80%, orange color solid). ^{1}H NMR (400 MHz $CDCl_3$): δ 10.02 (s, 1H), 8.60 (d, J = 8 Hz, 2H), 8.43 (s, 1 H), 8.01 (d, J = 8 Hz, 2H), 7.91 (m, 2H), 7.85 (m, 2H), 7.74 (m, 4H), 7.62 (m, 2H), 7.53 (m, 2H). ^{13}C NMR (100 MHz $CDCl_3$) 191.4, 135.5, 133.9, 133.7, 132.8, 132.1, 131.2, 129.7, 128.9, 128.7, 127.0, 126.5, 125.8, 116.3, 99.9, 90.6. HRMS: $[M + H]^+$ calcd for $C_{23}H_{15}O$, 307.1117; found $[M + H]^+$, 307.1117.

Synthesis of 5. Compound **5** was prepared following a procedure similar to that used for compound **4**. The quantities involved and characterization data are shown below; 4-Ethynylbenzaldehyde (0.5 g, 3.84 mmol), 9,10 dibromoanthracene (0.54 g, 1.61 mmol), CuI (0.058 g, 0.31 mmol), and $Pd(PPh_3)_2Cl_2$ (0.13 g, 0.09 mmol) in dry triethylamine (25 mL) and THF (40 mL). Yield: 72%. ^{1}H NMR (400 MHz $CDCl_3$): δ 10.09 (s, 2H), 8.68 (m, 4H), 7.98 (d, J = 8 Hz, 4H), 7.93 (d, J = 8 Hz, 4H), 7.69 (m, 4H). ^{13}C NMR (100 MHz $CDCl_3$) 191.4, 135.8, 132.3, 132.2, 129.8, 129.5, 127.4, 127.3, 118.5, 101.8, 90.4. HRMS: $[M + H]^+$ calcd for $C_{32}H_{19}O$, 435.1380; found $[M + H]^+$, 435.1370.

Synthesis of 6. Compound **6** was prepared following a procedure similar to that used for compound **4**. The quantities involved and characterization data are shown below; 4-Ethynylbenzaldehyde (0.5 g, 3.845 mmol), 9,10 dibromoanthracene (1.60 g, 4.81 mmol), CuI (0.058 g, 0.31 mmol), and $Pd(PPh_3)_2Cl_2$ (0.13 g, 0.09 mmol) in dry triethylamine (25 mL) and THF (40 mL). Yield: 75%. ^{1}H NMR (400 MHz $CDCl_3$): δ 10.07 (s, 1H), 8.63 (m, 2H), 8.56 (m, 2 H), 7.94 (d, J = 8 Hz, 2H), 7.88 (d, J = 8 Hz, 2H), 7.64 (m, 4H). ^{13}C NMR (100 MHz $CDCl_3$) 191.4, 135.7, 134.1, 133.1, 132.1, 130.3, 129.5, 128.4, 127.6, 127.2, 126.9, 125.4, 117.2, 100.7, 90.7. HRMS: $[M + H]^+$ calcd for $C_{23}H_{14}OBr$, 385.0228; found $[M + H]^+$, 385.0304.

■ ASSOCIATED CONTENT

Supporting Information

The Supporting Information is available free of charge on the ACS Publications website at DOI: 10.1021/acsomega.8b01142.

Characterization of target compounds; sensing studies; comparison of detection limits with reported data; DFT data; LOD and LOQ for 1−3; comparison of detection limits of the present work with other reported values; determination of Hg^{2+} in real samples; and computational results of optimized structure of 1, 1 + Hg^{2+}, 2, 2 + Hg^{2+}, 3, and 3 + Hg^{2+} (PDF)

■ AUTHOR INFORMATION

Corresponding Authors

*E-mail: swamy@technion.ac.il (C.a.s.P.)
*E-mail: raman474@gmail.com (G.S.)

ORCID

Chinna ayya swamy P: 0000-0001-7875-9517
Subramanian Singaravadivel: 0000-0001-5554-8522
Gandhi Sivaraman: 0000-0002-6919-9658

Notes

The authors declare no competing financial interest.

■ ACKNOWLEDGMENTS

S.S thanks the DST-SERB Early Career Research Award for financial support (no. ECR/2017/000380/CS).

■ REFERENCES

(1) (a) Carter, K. P.; Young, A. M.; Palmer, A. E. Fluorescent Sensors for Measuring Metal Ions in Living Systems. *Chem. Rev.* **2014**, *114*, 4564−4601. (b) Sareen, D.; Kaur, P.; Singh, K. Strategies in detection of metal ions using dyes. *Coord. Chem. Rev.* **2014**, *265*, 125−154. (c) Nolan, E. M.; Lippard, S. J. Tools and Tactics for the Optical Detection of Mercuric Ion. *Chem. Rev.* **2008**, *108*, 3443−3480.

(2) (a) Park, J.-D.; Zheng, W. Human Exposure and Health Effects of Inorganic and Elemental Mercury. *J. Prev. Med. Public Health* **2012**, *45*, 344−352. (b) Wang, S.; Shi, X. Molecular mechanisms of metal toxicity and carcinogenesis. *Mol. Cell. Biochem.* **2001**, *222*, 3−9. (c) Tchounwou, P. B.; Yedjou, C. G.; Patlolla, A. K.; Sutton, D. J. Heavy Metal Toxicity and the Environment. *Experientia Suppl.* **2012**, *101*, 133−164.

(3) Reducing Mercury in Artisanal and Small-Scale Gold Mining (ASGM), United Nations Environment Programme. http://web.unep.org/chemicalsandwaste/global-mercury-partnership/reducing-mercury-artisanal-and-small-scale-gold-mining-asgm (accessed 10 October 2017). (b) UNEP. *Global Mercury Assessment 2013: Sources, Emissions, Releases and Environmental Transport*; UNEP Chemicals Branch: Geneva, Switzerland, 2013.

(4) (a) Onyido, I.; Norris, A. R.; Buncel, E. Biomolecule−Mercury Interactions. Modalities of DNA Base−Mercury Binding Mechanisms. Remediation Strategies. *Chem. Rev.* **2004**, *104*, 5911−5930. (b) Harris, H. H.; Pickering, I. J.; George, G. N. The Chemical Form of Mercury in Fish. *Science* **2003**, *301*, 1203.

(5) (a) Motaharian, A.; Motaharian, F.; Abnous, K.; Hosseini, M. R. M.; Hassanzadeh-Khayyat, M. Molecularly imprinted polymer nanoparticles-based electrochemical sensor for determination of diazinon pesticide in well water and apple fruit samples. *Anal. Bioanal. Chem.* **2016**, *408*, 6769−6779. (b) Gao, Y.; De Galan, S.; De Brauwere, A.; Baeyens, W.; Leermakers, M. Mercury speciation in hair by headspace injection−gas chromatography−atomic fluorescence spectrometry (methylmercury) and combustion-atomic absorption spectrometry (total Hg). *Talanta* **2010**, *82*, 1919−1923. (c) Moreno, F.; Garcia-Barrera, T.; Gomez-Ariza, J. L. Simultaneous analysis of mercury and selenium species including chiral forms of selenomethionine in human urine and serum by HPLC column-switching coupled to ICP-MS. *Analyst* **2010**, *135*, 2700−2705. (d) Krishna, M. V. B.; Chandrasekaran, K.; Karunasagar, D. On-line speciation of inorganic and methyl mercury in waters and fish tissues using

DOI: 10.1021/acsomega.8b01142
ACS Omega 2018, 3, 12341−12348

polyaniline micro-column and flow injection-chemical vapour generation-inductively coupled plasma mass spectrometry (FI-CVG-ICPMS). *Talanta* **2010**, *81*, 462−472. (e) Chai, X.; Chang, X.; Hu, Z.; He, Q.; Tu, Z.; Li, Z. Solid phase extraction of trace Hg(II) on silica gel modified with 2-(2-oxoethyl)hydrazine carbothioamide and determination by ICP-AES. *Talanta* **2010**, *82*, 1791−1796.

(6) (a) Lee, Y. H.; Liu, H.; Lee, J. Y.; Kim, S. H.; Kim, S. K.; Sessler, J. L.; Kim, Y.; Kim, J. S. Dipyrenylcalix[4]arene—A Fluorescence-Based Chemosensor for Trinitroaromatic Explosives. *Chem.—Eur. J.* **2010**, *16*, 5895−5901. (b) Germain, M. E.; Knapp, M. J. Optical explosives detection. from color changes to fluorescence turn-on. *Chem. Soc. Rev.* **2009**, *38*, 2543−2555.

(7) (a) Arivazhagan, C.; Borthakur, R.; Ghosh, S. Ferrocene and Triazole-Appended Rhodamine Based Multisignaling Sensors for Hg2+ and Their Application in Live Cell Imaging. *Organometallics* **2015**, *34*, 1147−1155. (b) Vengaian, K. M.; Britto, C. D.; Sivaraman, G.; Sekar, K.; Singaravadivel, S. Phenothiazine based sensor for naked-eye detection and bioimaging of Hg(II) and F− ions. *RSC Adv.* **2015**, *5*, 94903−94908. (c) Caballero, A.; Martínez, R.; Lloveras, V.; Ratera, I.; Vidal-Gancedo, J.; Wurst, K.; Tárraga, A.; Molina, P.; Veciana, J. Highly Selective Chromogenic and Redox or Fluorescent Sensors of Hg2+ in Aqueous Environment Based on 1,4-Disubstituted Azines. *J. Am. Chem. Soc.* **2005**, *127*, 15666−15667. (d) Hussain, M. M.; Rahman, M. M.; Arshad, M. N.; Asiri, A. M. Hg2+ Sensor Development Based on (E)-N′-Nitrobenzylidene-Benzenesulfonohydrazide (NBBSH) Derivatives Fabricated on a Glassy Carbon Electrode with a Nafion Matrix. *ACS Omega* **2017**, *2*, 420−431. (e) Arshad, M. N.; Rahman, M. M.; Asiri, A. M.; Sobahiab, T. R.; Yu, S.-H. Development of Hg^{2+} sensor based on N′-[1-(pyridin-2-yl)ethylidene]benzenesulfono-hydrazide (PEBSH) fabricated silver electrode for environmental remediation. *RSC Adv.* **2015**, *5*, 81275−81281. (f) Mahato, P.; Saha, A.; Das, A.; Agarwalla, H.; Das, A. An overview of the recent developments on Hg^{2+} recognition. *RSC Adv.* **2014**, *4*, 36140−36174.

(8) (a) Kim, H. N.; Ren, W. X.; Kim, J. S.; Yoon, J. Fluorescent and colorimetric sensors for detection of lead, cadmium, and mercury ions. *Chem. Soc. Rev.* **2012**, *41*, 3210−3244. (b) Yang, Y.-K.; Yook, K.-J.; Tae, J. A Rhodamine-Based Fluorescent and Colorimetric Chemodosimeter for the Rapid Detection of Hg2+ Ions in Aqueous Media. *J. Am. Chem. Soc.* **2005**, *127*, 16760−16761. (c) Saleem, M.; Lee, K. H. Optical sensor. a promising strategy for environmental and biomedical monitoring of ionic species. *RSC Adv.* **2015**, *5*, 72150−72287. (d) Chen, G.; Guo, Z.; Zeng, G.; Tang, L. Fluorescent and colorimetric sensors for environmental mercury detection. *Analyst* **2015**, *140*, 5400−5443. (e) Yan, Z.; Yuen, M.-F.; Hu, L.; Sun, P.; Lee, C.-S. Advances for the colorimetric detection of Hg2+ in aqueous solution. *RSC Adv.* **2014**, *4*, 48373−48388. (f) Khan, A.; et al. Sol−gel synthesis and characterization of conducting polythiophene/tin phosphate nano tetrapod composite cation-exchanger and its application as Hg(II) selective membrane electrode. *J. Sol-Gel Sci. Technol.* **2013**, *65*, 160−169. (g) Hussein, M. A.; Rahman, M. M.; Asiri, A. M. Novel Facial Conducting Polyamide-Based Dithiophenylidene Cyclyhexanone Moiety Utilized for Selective Cu2+ Sensing. *Polym.-Plast. Technol. Eng.* **2018**, *57*, 812−825. (h) Sharma, H.; Kaur, N.; Singh, A.; Kuwar, A.; Singh, N. Optical chemosensors for water sample analysis. *J. Mater. Chem. C* **2016**, *4*, 5154−5194.

(9) (a) Ding, J.; Li, H.; Xie, Y.; Peng, Q.; Li, Q.; Li, Z. Reaction-based conjugated polymer fluorescent probe for mercury(II). good sensing performance with "turn-on" signal output. *Polym. Chem.* **2017**, *8*, 2221−2226. (b) Cheng, X.; Li, S.; Jia, H.; Zhong, A.; Zhong, C.; Feng, J.; Qin, J.; Li, Z. Fluorescent and Colorimetric Probes for Mercury(II). Tunable Structures of Electron Donor and π-Conjugated Bridge. *Chem.—Eur. J.* **2012**, *18*, 1691−1699. (c) Cheng, X.; Li, Q.; Li, C.; Qin, J.; Li, Z. Azobenzene-Based Colorimetric Chemosensors for Rapid Naked-Eye Detection of Mercury(II). *Chem.—Eur. J.* **2011**, *17*, 7276−7281. (d) Awual, R.; Hasan, M.; Eldesoky, G. E.; Khaleque, A.; Rahman, M. M.; Naushad, M. Facile mercury detection and removal from aqueous media involving ligand impregnated conjugate nanomaterials. *Chem. Eng. J.* **2016**, *290*, 243−251. (e) Xu, X.; Li, Y.-F.; Zhao, J.; Li, Y.; Lin, J.; Li, B.; Gao, Y.; Chen, C. Nanomaterial-based approaches for the detection and speciation of mercury. *Analyst* **2015**, *140*, 7841−7853. (f) Chen, X.; Baek, K.-H.; Kim, J.; Kim, S.-J.; Shin, I.; Yoon, J. A selenolactone-based fluorescent chemodosimeter to monitor mecury/methylmercury species in vitro and in vivo. *Tetrahedron* **2010**, *66*, 4016−4021.

(10) (a) Zhang, Z.; Zhang, B.; Qian, X.; Li, Z.; Xu, Z.; Yang, Y. Simultaneous Quantification of Hg2+ and MeHg+ in Aqueous Media with a Single Fluorescent Probe by Multiplexing in the Time Domain. *Anal. Chem.* **2014**, *86*, 11919−11924. (b) Jiang, W.; Wang, W. A selective and sensitive "turn-on" fluorescent chemodosimeter for Hg2+ in aqueous media via Hg^{2+} promoted facile desulfurization−lactonization reaction. *Chem. Commun.* **2009**, 3913−3915.

(11) (a) Gao, Y.; Ma, T.; Ou, Z.; Cai, W.; Yang, G.; Li, Y.; Xu, M.; Li, Q. Highly sensitive and selective turn-on fluorescent chemosensors for Hg2+ based on thioacetal modified pyrene. *Talanta* **2018**, *178*, 663−669. (b) Ruan, Y.; Shan, Y.; Gong, Y.; Wang, C.; Ye, C.; Qiu, Y.; Liang, Z.; Li, Z. Novel AIE-active ratiometric fluorescent probes for mercury(II) based on the Hg2+-promoted deprotection of thioketal, and good mechanochromic properties. *J. Mater. Chem. C* **2018**, *6*, 773−780. (c) Tang, Y.; Lee, D.; Wang, J.; Li, G.; Yu, J.; Lin, W.; Yoon, J. Development of fluorescent probes based on protection−deprotection of the key functional groups for biological imaging. *Chem. Soc. Rev.* **2015**, *44*, 5003−5015. (d) Xu, D.; Tang, L.; Tian, M.; He, P.; Yan, X. A benzothizole-based fluorescent probe for Hg2+ recognition utilizing ESIPT coupled AIE characteristics. *Tetrahedron Lett.* **2017**, *58*, 3654−3657. (f) Kumar, G. G. V.; et al. A reversible fluorescent chemosensor for the rapid detection of Hg2+ in an aqueous solution. Its logic gates behavior. *Sens. Actuators, B* **2018**, *273*, 305−315. (e) Song, K. C.; Kim, J. S.; Park, S. M.; Chung, K.-C.; Ahn, S.; Chang, S.-K. Fluorogenic Hg2+-Selective Chemodosimeter Derived from 8-Hydroxyquinoline. *Org. Lett.* **2006**, *8*, 3413−3416.

(12) Cheng, X.; Li, S.; Zhong, A.; Qin, J.; Li, Z. New fluorescent probes for mercury(II) with simple structure. *Sens. Actuators B Chem.* **2011**, *157*, 57−63.

(13) Guo, Y.; An, J.; Tang, H.; Peng, M.; Suzenet, F. Selective and "turn-off" fluorimetric detection of mercury(II) based on coumarinyldithiolane and coumarinyldithiane in aqueous solution. *Mater. Res. Bull.* **2015**, *63*, 155−160.

(14) Liu, K.; Xu, Z.; Yin, M.; Yang, W.; He, B.; Wei, W.; Shen, J. A multifunctional perylenediimide derivative (DTPDI) can be used as a recyclable specific Hg2+ ion sensor and an efficient DNA delivery carrier. *J. Mater. Chem. B.* **2014**, *2*, 2093−2096.

(15) (a) Xu, Q.-W.; Wang, C.; Sun, Z.-B.; Zhao, C.-H. A highly selective ratiometric bifunctional fluorescence probe for Hg2+ and F− ions. *Org. Biomol. Chem.* **2015**, *13*, 3032−3039. (b) Vedamalai, M.; Wu, S.-P. A BODIPY-Based Highly Selective Fluorescent Chemosensor for Hg2+ Ions and Its Application in Living Cell Imaging. *Eur. J. Org. Chem.* **2012**, 1158−1163.

(16) Yan, Y.; Che, Z.; Yu, X.; Zhi, X.; Wang, J.; Xu, H. Fluorescence "on-off-on" chemosensor for sequential recognition of Fe3+ and Hg2+ in water based on tetraphenylethylene motif. *Bioorg. Med. Chem.* **2013**, *21*, 508−513.

(17) Dai, H.; Yan, Y.; Guo, Y.; Fan, L.; Che, Z.; Xu, H. A Selective and Sensitive "Turn-on" Fluorescent Chemosensor for Recognition of Hg2+ Ions in Water. *Chem.—Eur. J.* **2012**, *18*, 11188−11191.

(18) Lu, Y.; Wang, J.; McGoldrick, N.; Cui, X.; Zhao, J.; Caverly, C.; Twamley, B.; ÓMáille, G. M.; Irwin, B.; Conway-Kenny, R.; Draper, S. M. Iridium(III) Complexes Bearing Pyrene-Functionalized 1,10-Phenanthroline Ligands as Highly Efficient Sensitizers for Triplet−Triplet Annihilation Upconversion. *Angew. Chem. Int. Ed.* **2016**, *55*, 14688−14692.

(19) Mukherjee, S.; Thilagar, P. Molecular flexibility tuned emission in "V" shaped naphthalimides. Hg(II) detection and aggregation-induced emission enhancement (AIEE). *Chem. Commun.* **2013**, *49*, 7292−7294.

(20) (a) Chen, T.; Zhu, W.; Xu, Y.; Zhang, S.; Zhang, X.; Qian, X. A thioether-rich crown-based highly selective fluorescent sensor for

DOI: 10.1021/acsomega.8b01142
ACS Omega 2018, 3, 12341−12348

Hg^{2+} and Ag^{+} in aqueous solution. *Dalton Trans.* **2010**, *39*, 1316−1320. (b) Gao, Y.; Zhang, C.; Peng, S.; Chen, H. A fluorescent and colorimetric probe enables simultaneous differential detection of Hg^{2+} and Cu^{2+} by two different mechanisms. *Sens. Actuators, B* **2017**, *238*, 455−461. (c) Cheng, X.; Li, S.; Jia, H.; Zhong, A.; Zhong, C.; Feng, J.; Qin, J.; Li, Z. cπ-Conjugated Bridge. *Chem.−Eur. J.* **2012**, *18*, 1691−1699.

(21) Zhang, X.; Xu, Y.; Guo, P.; Qian, X. A dual channel chemodosimeter for Hg2+ and Ag+ using a 1,3-dithiane modified BODIPY. *New J. Chem.* **2012**, *36*, 1621−1625.

(22) Koteeswari, R.; Ashokkumar, P.; Malar, E. J. P.; Ramakrishnan, V. T.; Ramamurthy, P. Highly selective, sensitive and quantitative detection of Hg2+ in aqueous medium under broad pH range. *Chem. Commun.* **2011**, *47*, 7695−7697.

(23) Risch, M. J.; Trucks, G. W.; Schlegel, H. B.; Scuseria, G. E.; Robb, M. A.; Cheeseman, J. R.; Scalmani, G.; Barone, V.; Mennucci, B.; Petersson, G. A.; Nakatsuji, H.; Caricato, M.; Li, X.; Hratchian, H. P.; Izmaylov, A. F.; Bloino, J.; Zheng, G.; Sonnenberg, J. L.; Hada, M.; Ehara, M.; Toyota, K.; Fukuda, R.; Hasegawa, J.; Ishida, M.; Nakajima, T.; Honda, Y.; Kitao, O.; Nakai, H.; Vreven, T.; Montgomery, J. A., Jr; Peralta, J. E.; Ogliaro, F.; Bearpark, M.; Heyd, J. J.; Brothers, E.; Kudin, K. N.; Staroverov, V. N.; Kobayashi, R.; Normand, J.; Raghavachari, K.; Rendell, A.; Burant, J. C.; Iyengar, S. S.; Tomasi, J.; Cossi, M.; Rega, N.; Millam, J. M.; Klene, M.; Knox, J. E.; Cross, J. B.; Bakken, V.; Adamo, C.; Jaramillo, J.; Gomperts, R.; Stratmann, R. E.; Yazyev, O.; Austin, A. J.; Cammi, R.; Pomelli, C.; Ochterski, J. W.; Martin, R. L.; Morokuma, K.; Zakrzewski, V. G.; Voth, G. A.; Salvador, P.; Dannenberg, J. J.; Dapprich, S.; Daniels, A. D.; Farkas, O.; Foresman, J. B.; Ortiz, J. V.; Cioslowski, J.; Fox, D. J. *Gaussian 09*, Revision A.02; Gaussian Inc: Wallingford CT, 2009.

(24) (a) Otwinowski, Z.; Minor, W. Processing of X-ray diffraction data collected in oscillation mode. *Methods Enzymol.* **1997**, *276*, 307−326. (b) Mackay, S.; Gilmore, C. J.; Edwards, C.; Tremayne, M.; Stuart, N.; Shankland, K.; Xus, M. A. "*A computer program for the solution and refinement of crystal structures from diffraction data*"; University of Glasgow: Scotland, U.K., Nonius BV, Delft, The Netherlands and MacScience Co. Ltd., Yokohama, Japan, 1998.

(25) Sheldrick, G. M. *Program for the Refinement of Crystal Structures; SHELXL97*; University of Gottingen: Germany, 1997.

DOI: 10.1021/acsomega.8b01142
ACS Omega 2018, 3, 12341−12348